

Manipulating microbending losses in single mode optical fiber for pressure sensing

Open
Access

Wan Maisarah Mukhtar^{1,*}, Nur Auni Marzuki¹, Affa Rozana Abdul Rashid¹

¹ Faculty of Science and Technology, Universiti Sains Islam Malaysia, 71800 Bandar Baru Nilai, Negeri Sembilan, Malaysia

ARTICLE INFO

ABSTRACT

Article history:

Received 28 August 2017

Received in revised form 26 October 2017

Accepted 2 November 2017

Available online 8 November 2017

This paper reports the effect of microbending losses in single mode optical fiber for pressure sensing system application. Several types of periodical corrugated plates were fabricated, namely cylindrical-structured surface (Plate A) and rectangular-structured surface (Plate B) with thicknesses of corrugated parts were varied at 0.1 cm, 0.2 cm and 0.3 cm. Laser sources with excitation wavelengths of $\lambda_1=1310$ nm and $\lambda_2=1550$ nm were launched at the first end of the fiber. The values of losses were recorded by using an optical power meter. It was clearly seen that the microbending losses were polynomially increased with the increment of applied pressure and the thicknesses of corrugated parts of Plate A and Plate B. The maximum microbending losses of 1.5185 dBm/kPa was resulted as SMF was coupled with corrugated plates B with thicknesses of 0.3cm by using excitation wavelength of 1550nm. These values reduced to 0.7628 dBm/kPa and 0.4014 dBm/kPa as the thicknesses were decreased to 0.2cm and 0.1cm respectively. In comparison with a plain plate which acted as a reference indicator, the maximum percentage of microbending losses was obtained as 74.29 % for Plate A and 95.02 % for Plate B. In conclusions, we successfully proved the ability of SMF as a pressure sensor by manipulating the microbending losses experienced by the fiber. The employment of 1550nm of laser wavelength results better sensitivity sensor where the system able to detect large losses as the pressure applied on the corrugated surfaces.

Keywords:

Microbending loss, corrugated plate, single mode fiber, fiber optic pressure sensing system

Copyright © 2017 PENERBIT AKADEMIABARU - All rights reserved

1. Introduction

Quality constructions in structural engineering affect many aspects such as human and economical of our societies [1]. Due to the lifetime factors, most of structures such as building, tunnel and bridge are potential to be exposed to the damage which induce by environmental degradation such as cracking and aging [2]. Daily overload also results the deterioration of structural design. The

* Corresponding author.

E-mail address: [Wan Maisarah Mukhtar \(wmaisarah@usim.edu.my\)](mailto:wmaisarah@usim.edu.my)

structural failure will consequence the society' safety. To overcome this issue, sensors for health monitoring system have been introduced [3-5].

There are many types of sensors such as mechanical sensors [6-7], electronic sensors [8-9] and optical sensors [10-13] which have been used to detect building cracks. However, the disadvantages of mechanical and electronic sensors are due to their low sensitivity, delicate properties and complicated design structures [14]. Recently, the application of optical sensors growth rapidly by considering its simplicity, high sensitivity, robust, easy-handling and safety [15-18]. Applications of optical fibers in sensing field were highlighted in many different areas such as in electrical power industry, medicine and in the field of oil and gas industry for monitoring of pipe line [19-23]. In health monitoring system, optical fibers have been appointed as an important medium to detect cracking issue by monitoring the bending losses of optical fiber [24-28].

Bending loss can be classified into two types such as microbending loss and macrobending loss. Macrobending loss happens when the fiber bends in a large radius of curvature compare to fiber diameter. Light will be absorbed by the cladding because the light strike core/cladding at radius less than critical angle. Microbending loss is repetitive small-scale fluctuations in the radius of curvature of the fiber axis. An increase in attenuation results from microbending because of the fiber curvature causes repetitive coupling of energy between the guided modes and the leaky modes in the fiber [29]. One of the challenge in structural health monitoring is to detect minor or small cracking area. The development of microbending loss based-fiber optics sensor that able to locate the existence of problematic area is expected can solve this issue.

In this study, we developed a pressure sensing system by employing two corrugated plates which were sandwiched between single mode fiber. The microbending losses were manipulated as main indicator in detecting the presence of applied pressure on the periodical corrugated surfaces.

2. Materials and Methods

Figure 1 displays an experimental setup of this work. A single mode optical fiber (SMF) with length of 200cm was connected in between laser source (Model: CSS1-SM (Noyes)) and optical power meter (Model: CSM1 (Noyes)). At a distance of $d_1 = 93.75\text{cm}$ from the laser source, an optical fiber was sandwiched with two types of corrugated plates structures namely Plate A and Plate B. Those plates consisted of cylindrical and rectangular corrugated structures respectively. The width of each rectangular corrugated part on Plate B was set at 0.01cm. Both plates have the same dimension of plate area which was width x length x thickness = 12.5 cm x 7.9 cm x 1.2 cm (Figure 2). The thicknesses for both corrugated parts were varied at 0.1 cm, 0.2 cm and 0.3 cm as listed in Table 1.

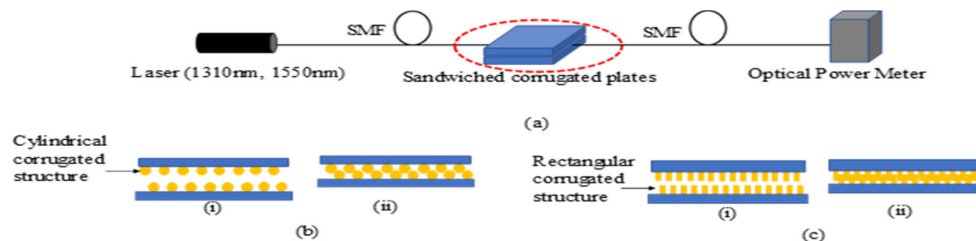


Fig. 1. (a) Experimental setup which consists of laser (excitation wavelength 1310nm and 1550nm), single mode fiber as light medium propagation, sandwiched corrugated plates which consists two type of plates and optical power meter to measure the optical losses due to the microbending factors; (b) Zoom-in the the sandwiched corrugated plates for Plate A (cylindrical structures) (i) before two surfaces were bring in contact (ii) after the surfaces were bring in contact; (c) Zoom-in the the sandwiched corrugated plates for Plate B (rectangular structures) (i) before two surfaces were bring in contact (ii) after the surfaces were bring in contact

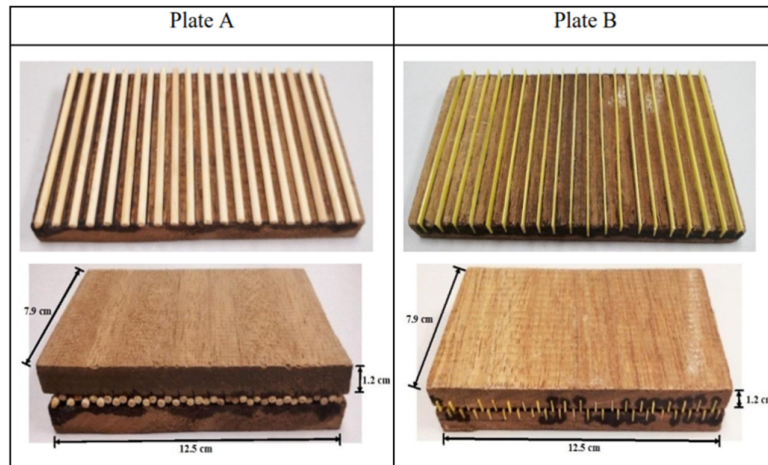

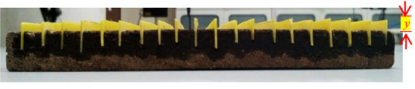


Fig. 2. Dimensions of corrugated plate A and plate B

Table 1
 Structures of Plate A and Plate B

Type of corrugated plate		Thickness of corrugated, y (cm)
Plate A		0.1
		0.2
		0.3
Plate B		0.1
		0.2
		0.3

The excitation wavelengths were varied at 1310nm and 1550nm to observe the influence of wavelength on the losses. A reference reading was recorded by measuring the optical power loss of SMF on a plain plate. To investigate the effect of applied pressure on the output of optical signal, the SMF was sandwiched between the plain plates to obtain reference values. The effect of pressure on the optical losses were studied by varies the load of masses on top of the plates from 1kg until 4kg with an increment of 1kg for each reading. The fiber's end was connected to the optical power meter to detect optical power losses which represents the microbending losses experienced by the stressed optical fiber. Next, the same procedure was repeated by using corrugated plate A and plate B to study the influence of corrugated plates structures with various applied pressure on the SMF microbending losses.

3. Results and Discussion

Figure 3 indicates the relationship between microbending losses, M_{loss} and applied pressure, P by using excitation wavelength of $\lambda_1=1310\text{nm}$ (Figure 3(a)) and $\lambda_2=1550\text{nm}$ (Figure 3(b)) as the SMF was sandwiched between two cylindrical corrugated plates. The circle-dotted lines represent references values where the SMF was located on the plain plate. The data was analyzed by performing a curve fitting method. It was clearly seen that the microbending losses were polynomially increased with the increment of applied pressure applied as shown by the dashed-lines. The greater the thicknesses of corrugated plates, the larger the losses resulted. The relationship between both parameters for excitation wavelength of $\lambda=1310\text{nm}$ (Figure 3(a)) can be interpreted as follows:

$$M_{loss} = 0.0064P^2 + 0.0144P + 1.3568, \text{ for } \gamma=0.1\text{cm} \quad (1)$$

$$M_{loss} = 0.0125P^2 + 0.0487P + 1.3435, \text{ for } \gamma=0.2\text{cm} \quad (2)$$

$$M_{loss} = 0.0424P^2 + 0.0639P + 1.3568, \text{ for } \gamma=0.3\text{cm} \quad (3)$$

where M_{loss} = microbending loss and P = applied pressure. The range of microbending losses for the three thicknesses of corrugated plates were between 1.36 dBm and 2.32 dBm. The graph's gradients were determined by calculated the tangential for each polynomial curve. The gradients became larger as the thicknesses of corrugated surfaces increased. At $\gamma=0.1\text{cm}$, the gradient was obtained as 0.0381 dBm/kPa. As the thickness of corrugated plate A was increased to $\gamma=0.2\text{ cm}$, the gradient of the graph increased to 0.0927 dBm/kPa. The employment of sandwiched corrugated plate A with $\gamma=0.3\text{cm}$ between the SMF exhibits large losses where the graph's gradient was obtained as 0.2267 dBm/kPa. In comparison between $\gamma=0.1\text{cm}$ and $\gamma=0.3\text{ cm}$, the microbending losses per applied pressure were increased up to 83.19 % with the increment of corrugated part's thicknesses.

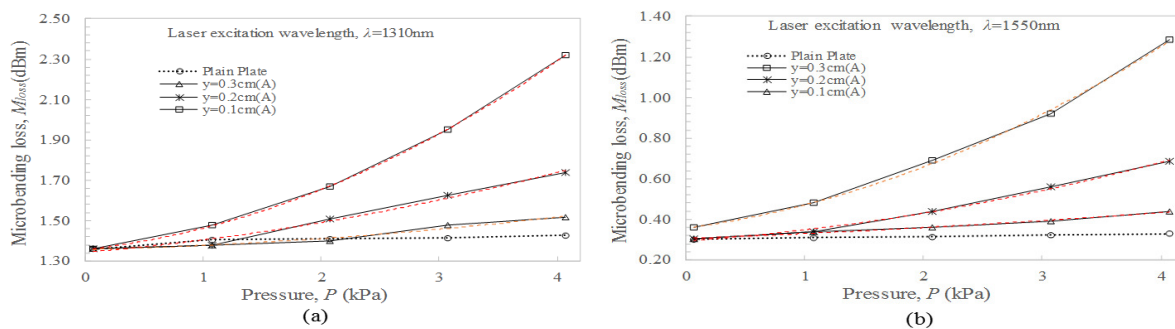


Fig. 3. Microbending losses experienced by SMF which were sandwiched between various thicknesses of corrugated plates A, γ by using laser with excitation wavelength, (a) $\lambda=1310\text{nm}$ (b) $\lambda=1550\text{nm}$

Similar pattern was observed as the laser excitation was replaced with 1550nm as portrays in Figure 3(b). The relationship between losses and applied pressure were obtained as follows:

$$M_{loss} = 0.0026P^2 + 0.0215P + 0.3057, \text{ for } \gamma=0.1\text{cm} \quad (4)$$

$$M_{loss} = 0.0143P^2 + 0.0395P + 0.2944, \text{ for } \gamma=0.2\text{cm} \quad (5)$$

$$M_{loss} = 0.0362P^2 + 0.0789P + 0.3560, \text{ for } \gamma=0.3\text{cm} \quad (6)$$

The range of microbending losses were between 0.300 dBm and 1.280 dBm. The employment of corrugated plate with $\gamma=0.1\text{ cm}$ indicated the smallest value of graph's gradient which is 0.0339 dBm/kPa. As γ was increased to 0.2 cm, the microbending loss was resulted as 0.0935 dBm/kPa. Meanwhile, the gradient of 0.2181 dBm/kPa was obtained with the appointment of corrugated plate with thickness of $\gamma=0.3\text{ cm}$. Obviously, the excitation wavelength gives significant impact on the

microbending losses where greater losses were resulted with an increment of 1.56% as the laser's wavelength was tuned into 1550nm.

The appointment of different corrugated pattern consisted of rectangular structures witnessed an obvious increment of microbending losses up to 80.60%. Figure 4(a) displays the characteristics of microbending losses as laser excitation wavelength was fixed at 1310nm where the SMF was sandwiched between plate B. Similar losses characteristics between corrugated plate A and B were obtained where the losses were increased with the increment of the corrugated part's thicknesses. At $\lambda=1310\text{nm}$ (Figure 4(a)), the SMF which was sandwiched between the corrugated plate B with thickness of 0.1cm; experienced small microbending loss presented by the slope of graph as 0.1186 dBm/kPa. The gradient of the graph reduced to 0.2233 dBm/kPa as the thickness of corrugated was increased to 0.2 cm. Maximum microbending loss about 3.25 dBm as the corrugated thickness was changed to $y=0.3\text{cm}$ in which resulted 0.4778 dBm/kPa of the value of graph's gradient. The minimum and maximum microbending losses using 1310nm of excitation wavelength were obtained as 1.36 dBm and 3.25 dBm respectively with percentage average losses were increased about 75.18% as thicknesses of the corrugated part increased. The relationship between applied pressure and microbending losses are expressed as follows:

$$M_{loss} = -0.01P^3 + 0.0571P^2 + 0.0472P + 1.3504, \text{ for } y=0.1\text{cm} \quad (7)$$

$$M_{loss} = -0.0158P^3 + 0.0919P^2 + 0.1039P + 1.3524, \text{ for } y=0.2\text{cm} \quad (8)$$

$$M_{loss} = -0.0392P^3 + 0.2661P^2 + 0.0311P + 1.3632, \text{ for } y=0.3\text{cm} \quad (9)$$

The microbending losses increased almost double (up to 6.62 dBm) as the laser excitation wavelength was tuned at 1550 nm as illustrated in Figure 4(b). The maximum microbending losses of 1.5185 dBm/kPa was resulted as the SMF was coupled with corrugated plates B with thicknesses of 0.3 cm. An increase in attenuation results from microbending due to fiber curvature causes repetitive coupling of energy between the guided modes and the leaky modes in the fiber [29]. The losses became smaller, where the data obtained were recorded as 0.7628 dBm/kPa and 0.4014 dBm/kPa when the thicknesses were decreased to 0.2cm and 0.1cm respectively. The mathematical expressions of the relationship between microbending losses and applied pressure are shown as below:

$$M_{loss} = -0.0175P^3 + 0.1444P^2 + 0.0847P + 0.4038, \text{ for } y=0.1\text{cm} \quad (10)$$

$$M_{loss} = -0.0483P^3 + 0.3837P^2 + 0.004P + 0.3796, \text{ for } y=0.2\text{cm} \quad (11)$$

$$M_{loss} = -0.0942P^3 + 0.7933P^2 + 0.1398P + 0.3821, \text{ for } y=0.3\text{cm} \quad (12)$$

Figure 5 depicts the normalized values of microbending losses by considering the differences between reference loss value and actual losses. The solid fill bars represent the usage of 1310nm as laser excitation wavelength. Meanwhile, 1550nm wavelength was indicated by the pattern fill bars. Both figures (Figure 5(a) and 5(b)) display similar characteristics where 1550nm results higher losses in comparison with 1310nm excitation wavelength. This phenomenon happens due to the

attenuation occur in the SMF as a result of light scattering and absorption and the presence of hydroxyl ion impurities [29]. The employment of Plate A obviously depicts minimum losses in comparison with Plate B due to its cylindrical structures which results smaller microbending. The SMF experienced strong microbending once it was coupled with the corrugated Plate B that consists of sharp rectangular shapes with width of 0.01cm. Microbending loss happens due to the external force that exert on the optical fiber that changes the propagation of light in optical fiber which resulted the optical power losses [30].

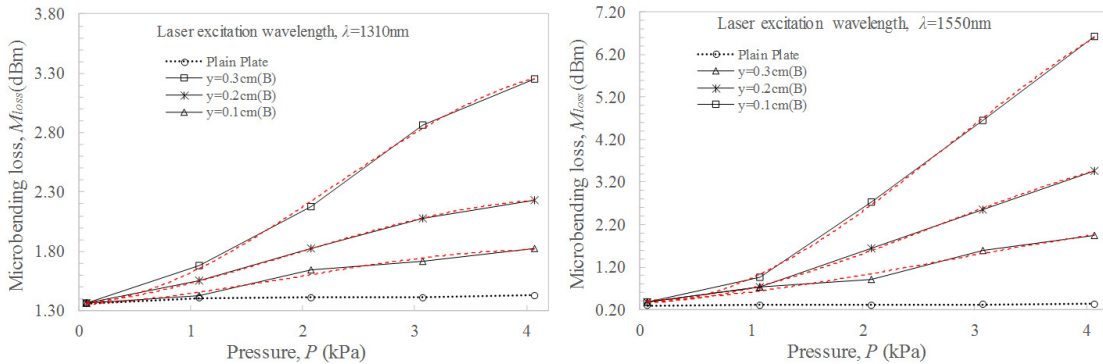


Fig. 4. Microbending losses experienced by SMF which were sandwiched between various thicknesses of corrugated plates B, y by using laser with excitation wavelength, (a) $\lambda=1310\text{nm}$ (b) $\lambda=1550\text{nm}$

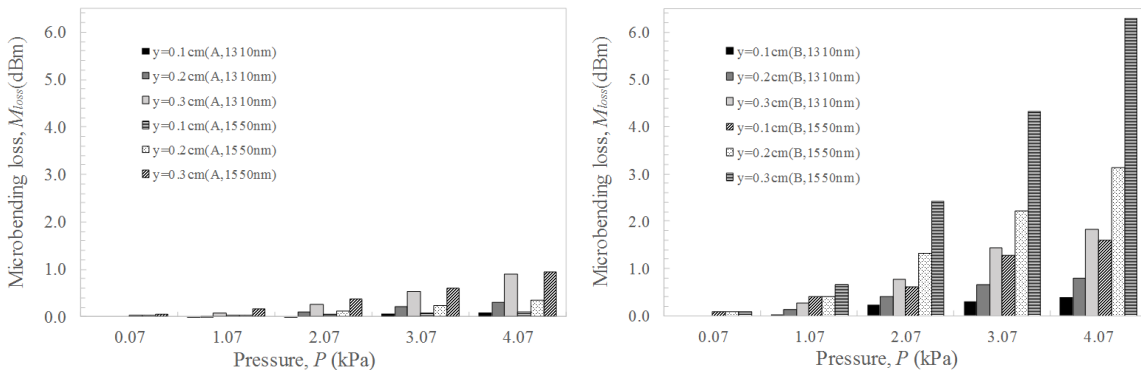


Fig. 5. Normalized microbending losses with various thicknesses of corrugated parts (a) Corrugated plate A (b) Corrugated plate B

4. Conclusion

This work proves the capability of fiber optic to be used as part of the pressure-sensing system. The microbending losses experience by the optical fiber can be manipulated to detect the surface roughness based on stress applied. High sensitivity sensor can be developed by controlling the laser excited wavelength. In comparison with 1310nm, the employment of 1550nm laser wavelength results better sensitivity sensor where the system able to detect large losses as the pressure applied on the corrugated surfaces. The interesting features of this sensor which are simple, low cost and high sensitivity demonstrates the versatility of fiber optic to be applied in structural monitoring system.

Acknowledgment

The work was supported by Universiti Sains Islam Malaysia (USIM) and Ministry of Higher Education (MOHE) under grant FRGS/2/2014/SG02/USIM/03/1.

References

- [1] López-Higuera, J.M., Cobo, L.R., Incera, A.Q. and Cobo, A., Fiber optic sensors in structural health monitoring. *Journal of Lightwave Technology* **29**, no. 4 (2011): 587-608.
- [2] Jusoh, S. N., H. Mohamad, A. Marto, NZ Mohd Yunus, F. Kasim, E. Namazi, and H. Sohaei. Precast Concrete Tunnel Segments: A Review on Current Research. *Journal of Advanced Review on Scientific Research* **6**, no. 1 (2015):16-27.
- [3] Bao, X. and Chen, L., Recent progress in distributed fiber optic sensors. *Sensors* **12**, no. 7 (2012): 8601-8639.
- [4] Mihailov, S.J., Fiber Bragg grating sensors for harsh environments. *Sensors* **12**, no. 2 (2012):1898-1918.
- [5] Anwar Zawawi, M., O'Keffe, S. and Lewis, E., Intensity-modulated fiber optic sensor for health monitoring applications: a comparative review. *Sensor Review* **33**, no. 1 (2013):57-67
- [6] Ham, S., Song, H., Oelze, M.L. and Popovics, J.S., A contactless ultrasonic surface wave approach to characterize distributed cracking damage in concrete. *Ultrasonics* **75**, (2017): 46-57.
- [7] Terasaki, N., Li, C., Zhang, L. and Xu, C.N., Active crack indicator with mechanoluminescent sensing technique: Detection of crack propagation on building. In *Sensors Applications Symposium (SAS)*, pp.1-5, 2012.
- [8] Alavi, A.H., Hasni, H., Lajnef, N. and Chatti, K., Continuous health monitoring of pavement systems using smart sensing technology. *Construction and Building Materials* **114**, (2017):719-736.
- [9] Laurinavičius, A., Paliukaitė, M., Motiejūnas, A., Žiliūtė, L. and Vaitkus, A., Monitoring the mechanical and structural behavior of the pavement structure using electronic sensors. *Computer-Aided Civil and Infrastructure Engineering* **30**, no. 4(2015):317-328.
- [10] Man, S.H., Chang, C.C., Hassan, M. and Bermak, A., Design and calibration of a wireless laser-based optical sensor for crack propagation monitoring. *Smart Structures and Systems* **15**, no. 6 (2015):1543-1567.
- [11] Zhang, N., Chen, W., Zheng, X., Hu, W. and Gao, M., Optical sensor for steel corrosion monitoring based on etched fiber Bragg grating sputtered with iron film. *IEEE Sensors Journal* **15**, no. 6 (2015):3551-3556.
- [12] Mukhtar, W.M., Shaari, S. and Menon, P.S., Propagation of surface plasmon waves at metal thin film/air interface using modified optical waveguiding assembly. *Optoelectron Adv.Mat.* **7**, (2013): 9-13.
- [13] Mukhtar, W.M., Shaari, S. and Menon, P.S., Influences of light coupling techniques to the excitation of surface plasmon polaritons. *Advanced Science Letters* **19**, no.1(2013):66-69.
- [14] Benbouzid, M.E.H., A review of induction motors signature analysis as a medium for faults detection. *IEEE transactions on industrial electronics* **47**, no.5 (2000):984-993.
- [15] Ascorbe, J., Corres, J.M., Matias, I.R. and Arregui, F.J., High sensitivity humidity sensor based on cladding-etched optical fiber and lossy mode resonances. *Sensors and Actuators B: Chemical* **233**, (2016):7-16.
- [16] Zhao, Y., Li, X.G., Zhou, X. and Zhang, Y.N., Review on the graphene based optical fiber chemical and biological sensors. *Sensors and Actuators B: Chemical* **231**, (2016):324-340.
- [17] Peters, K., Polymer optical fiber sensors—a review. *Smart materials and structures* **20**, no.1 (2010):013002.
- [18] Haroon, H. and Khalid, S. S., An overview of optical fiber sensor applications in liquid concentration measurements. *Journal of Advanced Review on Scientific Research* **36**, no. 1(2017): 1-7.
- [19] Wu, H., Luo, J., Wu, J., Liu, J., Lv, L., Rao, Y., Sun, X. and Atubga, D., Multi-point detection for polarization-sensitive optical time domain reflectometry and its applications in electric power industry. In *Progress in Electromagnetic Research Symposium (PIERS)*, pp. 4912-4918, 2016.
- [20] Witt, J., Narbonneau, F., Schukar, M., Krebber, K., De Jonckheere, J., Jeanne, M., Kinet, D., Paquet, B., Depre, A., D'Angelo, L.T. and Thiel, T., Medical textiles with embedded fiber optic sensors for monitoring of respiratory movement. *IEEE Sensors Journal* **12**, no.1(2012):246-254.
- [21] Taffoni, F., Formica, D., Saccomandi, P., Pino, G.D. and Schena, E., Optical fiber-based MR-compatible sensors for medical applications: An overview. *Sensors* **13**, no. 10(2013): 14105-14120.
- [22] Yamate, T., Fujisawa, G. and Ikegami, T., Optical sensors for the exploration of oil and gas. *Journal of Lightwave Technology* **35**, no.16(2017):3538-3545.
- [23] Wang, C., Olson, M., Doijkhand, N. and Singh, S., A novel DdTS technology based on fiber optics for early leak detection in pipelines. In *Security Technology (ICCST), 2016 IEEE International Carnahan Conference on IEEE*, pp.1-8, IEEE, 2016.

- [24] Chen, S.E., Smith, B. and Wang, P., Fiber optics sensing of stressing and fracture in cylindrical structures. *In Topics in Modal Analysis* **7**, (2014): 287-293, Springer, New York, NY.
- [25] Barrias, A., Casas, J.R. and Villalba, S., A review of distributed optical fiber sensors for civil engineering applications. *Sensors* **16**, no.5 (2016):748.
- [26] Mallik, N., Wali, A.S. and Kuri, N., Damage location identification through neural network learning from optical fiber signal for structural health monitoring. In *Proceedings of the 5th International Conference on Mechatronics and Control Engineering*, pp. 157-161, 2016.
- [27] Nakamura, A., Okamoto, K., Koshikiya, Y., Watanabe, H. and Manabe, T., Highly sensitive detection of microbending in single-mode fibers and its applications. *Optics Express* **25**, no. 5(2017): 5742-5748.
- [28] Ramakrishnan, M., Rajan, G., Semenova, Y. and Farrell, G., Overview of fiber optic sensor technologies for strain/temperature sensing applications in composite materials. *Sensors* **16**, no. 1(2016): 99.
- [29] Keiser, G., *Optical Fiber Communications*, McGrawHill Education, 2015.
- [30] Gasvik K. J., *Optical metrology*, John Wiley & Sons Ltd, 2002.